UNCLASSIFIED

Copy 7

~~CONFIDENTIAL~~

NASA TM X-760

NASA TM X-760

c.2

GROUP 4
Downgraded at 3 year intervals; declassified after 12 years

CLASSIFICATION CHANGED
UNCLASSIFIED
To ....
By authority of NASA LTR DTD Oct 21, 1969 / Date 7/10/70
3 Babel E. Smut

TECHNICAL MEMORANDUM

X-760

FLIGHT MEASUREMENTS OF VHF SIGNAL ATTENUATION AND ANTENNA IMPEDANCE FOR THE RAM A1 SLENDER PROBE AT VELOCITIES UP TO 17,800 FEET PER SECOND

By Theo E. Sims and Robert F. Jones

Langley Research Center
Langley Station, Hampton, Va.

NOFORN and USGA&C limitations removed per NASA TD 71-67 dtd 11/11/71, s/Gifford A. Young
9/30/2004

...SIFIED DOCUMENT - TITLE UNCLASSIFIED

NATIONAL AERONAUTICS AND SPACE ADMINISTRATION

WASHINGTON March 1963

~~CONFIDENTIAL~~

UNCLASSIFIED

UNCLASSIFIED

[redacted]

NATIONAL AERONAUTICS AND SPACE ADMINISTRATION

TECHNICAL MEMORANDUM X-760 [redacted].

FLIGHT MEASUREMENTS OF VHF SIGNAL ATTENUATION AND ANTENNA IMPEDANCE FOR THE RAM A1 SLENDER PROBE AT VELOCITIES UP TO 17,800 FEET PER SECOND*

By Theo E. Sims and Robert F. Jones

SUMMARY

A carefully controlled radio attenuation measurement experiment, RAM A1, was launched from NASA Wallops Station at 7:34 a.m. e.s.t. on August 30, 1961 and propelled to a peak velocity of 17,800 feet per second at an altitude of 176,000 feet. The payload stage was a slender probe with a 2-inch-diameter hemisphere nose followed by a 9° half-angle cone joined to a 9-inch-diameter cylindrical body and 10° half-angle flare section. Radio-frequency signal blackout was avoided by the use of this body shape. Attenuation of VHF signals from two antenna locations and voltage standing-wave ratio (VSWR) and antenna impedance for one antenna location were measured. The results of the flight are (1) the measured signal attenuations, a maximum of 25 decibels for the forward slot antenna and of 10 decibels for the aft ring antenna, lie within the predicted bounds according to the two limiting thermochemical-flow models, equilibrium flow and frozen flow, (2) the VSWR for the forward antenna rose to 8; this indicates a 4-decibel loss due to mismatch, (3) differences in signal loss from the forward slot antenna and the aft ring antenna may be due to either nonequilibrium chemistry in the flow field or greater detuning of the forward slot antenna which had narrow bandwidth characteristics, (4) antenna-pattern-shape changes due to the plasma sheath were small, (5) the forward-slot-antenna impedance shifted in the inductive direction, (6) the exhaust of the burning fourth-stage rocket had no apparent effect on VHF signal levels, and (7) attenuation of the signals received at Wallops when the slender probe was in the 300,000-foot-altitude region may be due to wake phenomena.

INTRODUCTION

Langley Research Center has designed a series of flight experiments that are referred to as Project RAM (Radio Attenuation Measurement) and are launched from NASA Wallops Station. The objective of the RAM experiments is to investigate the interference of ionized flow fields with communications, data transmission, and

---

*Title, Unclassified.

[redacted]

UNCLASSIFIED

radar tracking over a wide range of altitudes and velocities. This report describes the first project flight, hereinafter referred to as RAM A1. The letter designates the launch vehicle which was an NASA four-stage vehicle and the numeral refers serially to the experiment. The vehicle was launched at 7:34 a.m. e.s.t. on August 30, 1961.

The ionized-flow-field problem being investigated is illustrated in figure 1. The shaded area in the figure is the VHF blackout region (greater than 50 decibels) exhibited by numerous flights of blunt vehicles from Cape Canaveral and several NASA Wallops flights. The solid line in the figure is the RAM A1 velocity-altitude profile.

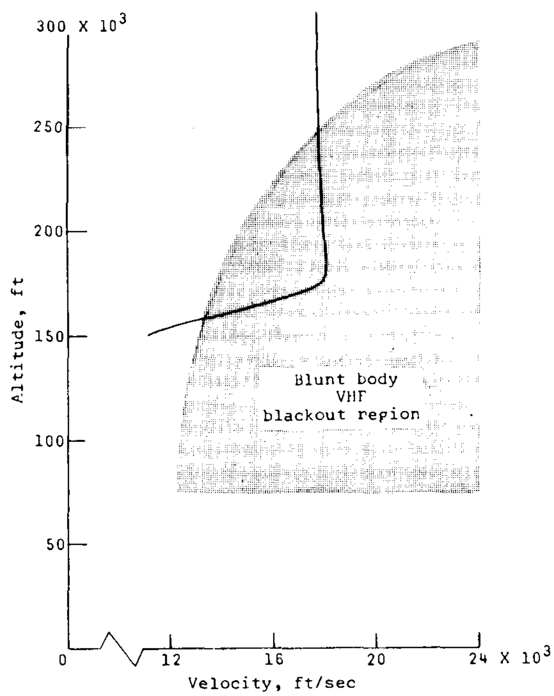

Figure 1.- Ram A1 velocity-altitude profile.

The RAM A1 experiment was designed to make a significant penetration of the VHF blackout region with only a medium signal loss. The purpose of the flight was to conduct a carefully controlled radio attenuation experiment to evaluate present prediction capabilities of transmission loss through reentry plasmas by using available flow-field and electromagnetic theories. The experiment was conducted during the ascending portion of the trajectory, which is essentially the reentry corridor in reverse. There are several advantages to an ascending trajectory: heat survival problems are minimized, the experiment is conducted close to the launch site insuring good radar tracking data and strong telemetry signals, and instrumentation performance may be checked before and after the data collecting period. A peak velocity of 17,800 feet per second was reached at an altitude of approximately 176,000 feet.

Also in this report, the radio attenuation data obtained at a point near maximum signal loss are compared with theoretical predictions in which equilibrium and frozen thermochemical-flow models are assumed.

PROBE DESCRIPTION

The four-stage solid-propellant rocket vehicle used to obtain the desired probe trajectory was designed by the Langley Research Center and is described in reference 1. The probe is shown in figure 2. It was a body of revolution 147 inches long with a 2-inch-diameter hemispherically blunted 9° half-angle conical nose, a 9-inch-diameter cylindrical midsection, and a 10° half-angle flare section at the rear. This slender cone-cylinder-flare body was used to avoid

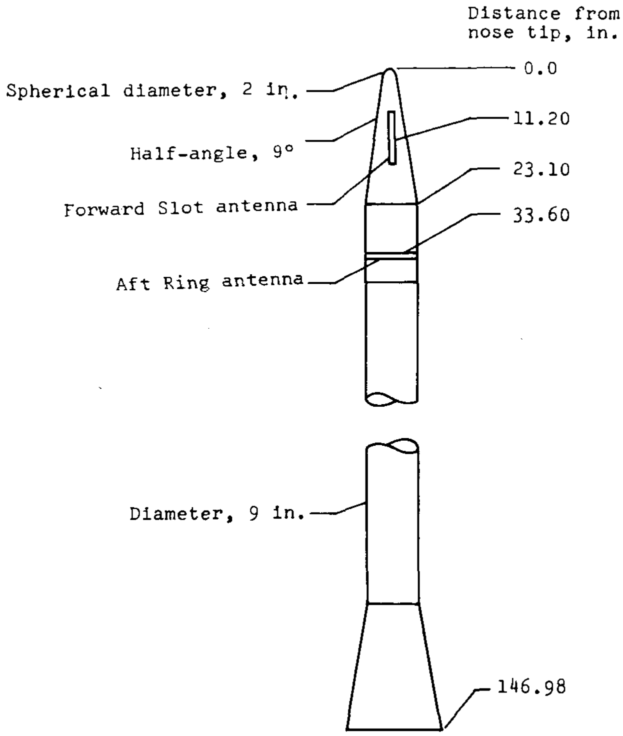

Figure 2.- Sketch of slender probe.

VHF signal blackout and to permit the use of available real gas solutions to make theoretical predictions of signal attenuation. The nose cone was made of all-metallic, heat-sink materials and was designed to withstand the high temperatures of the flight without contaminating the flow field with ablation products. The probe was carefully designed for both static and dynamic stability to insure a low angle of incidence during the data collecting period. Some coning during fourth-stage-rocket burning was anticipated because the free jet expansion of a rocket exhaust at high altitude can induce separated flow along the vehicle and cause a loss of aerodynamic stability (ref. 2).

Additional details on the probe may be obtained from reference 1.

INSTRUMENTATION

Probe

Two VHF antennas were used in the experiment. (See fig. 2.) The forward slot antenna was on the conical section of the probe and was used with a 244.3-mc continuous-wave (CW) transmitter. The aft ring antenna was on the cylindrical section of the probe and was used with a 240.2-mc telemeter. The dielectric separator for both antennas was aluminum oxide (Al_2O_3). The horizontal and vertical patterns for the forward slot antenna are shown in figure 3 and pertinent construction details are given in figure 4. Two slot antennas and an isolator or partition were designed into the probe but subsequent measurements demonstrated that only one slot antenna was necessary to obtain adequate pattern coverage; therefore, only one slot antenna was used during the flight. The patterns for the aft ring antenna are shown in figure 5 and significant construction details are given in figure 6. Bandwidth characteristics of the two antennas are given in figure 7.

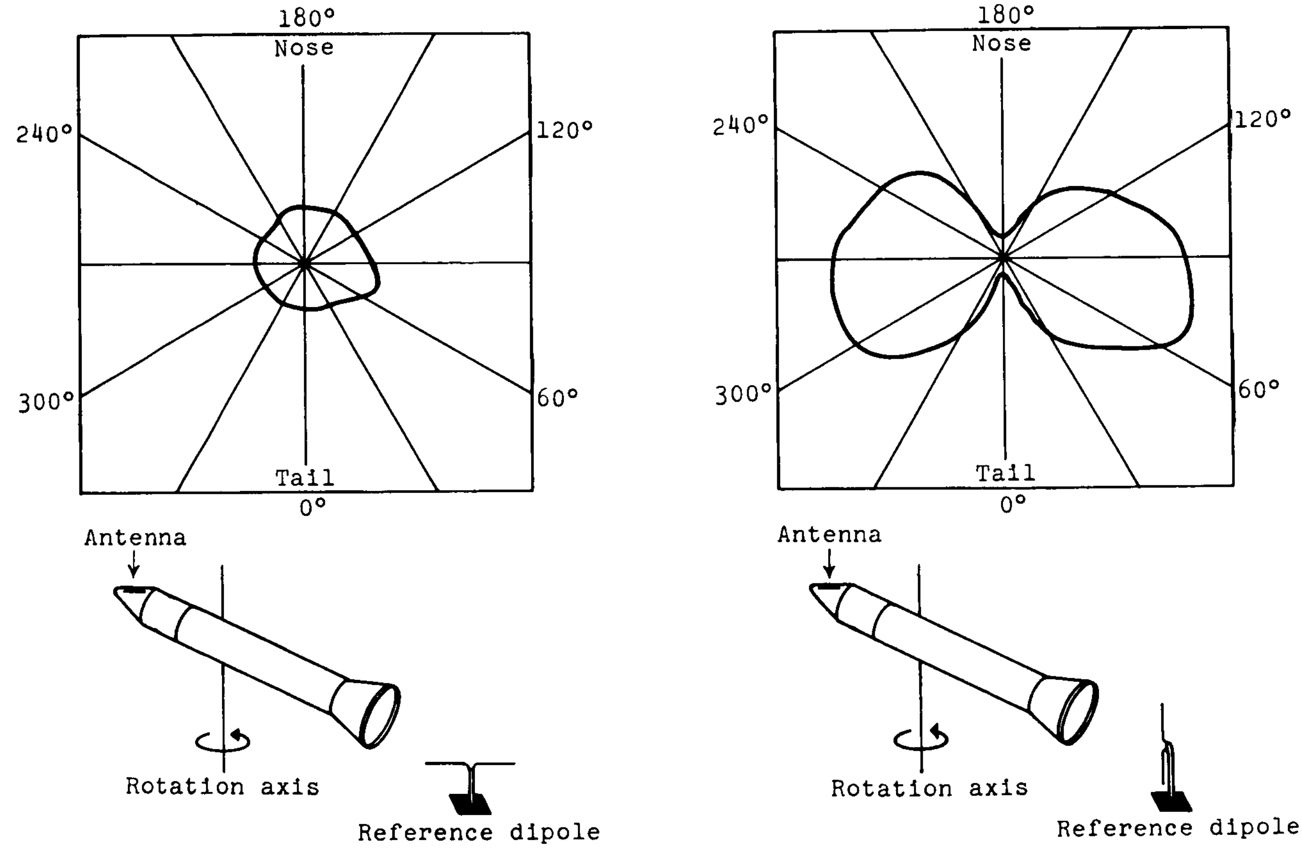

Figure 3.- Forward-slot-antenna pattern.

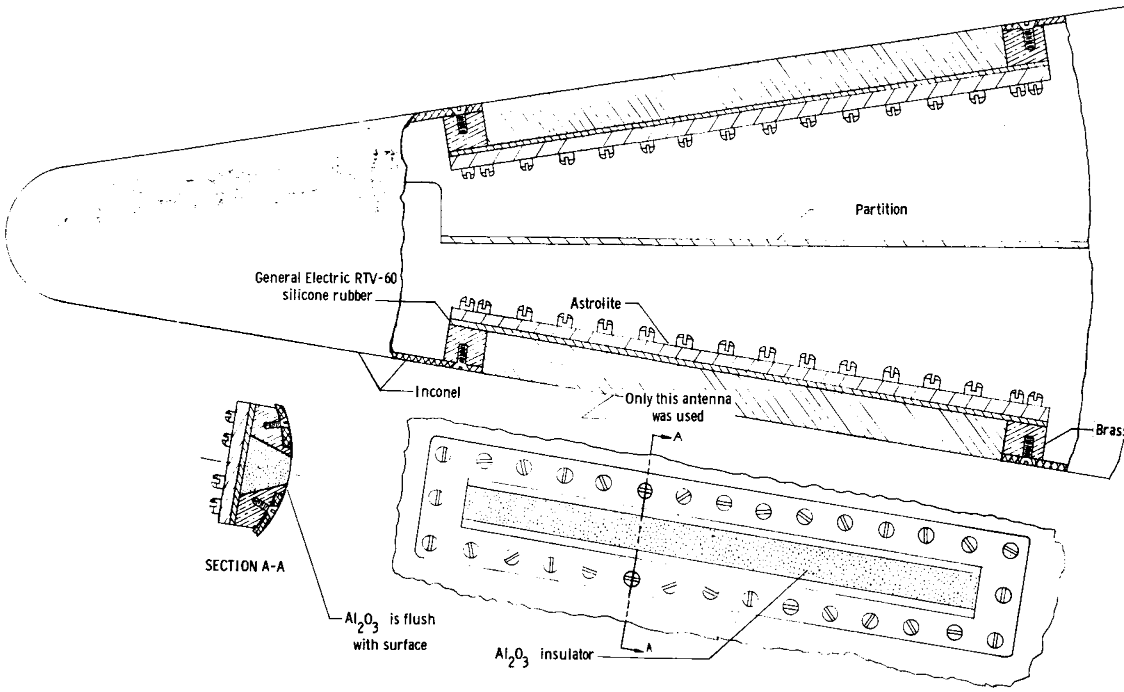

Figure 4.- Detail of forward-slot-antenna construction.

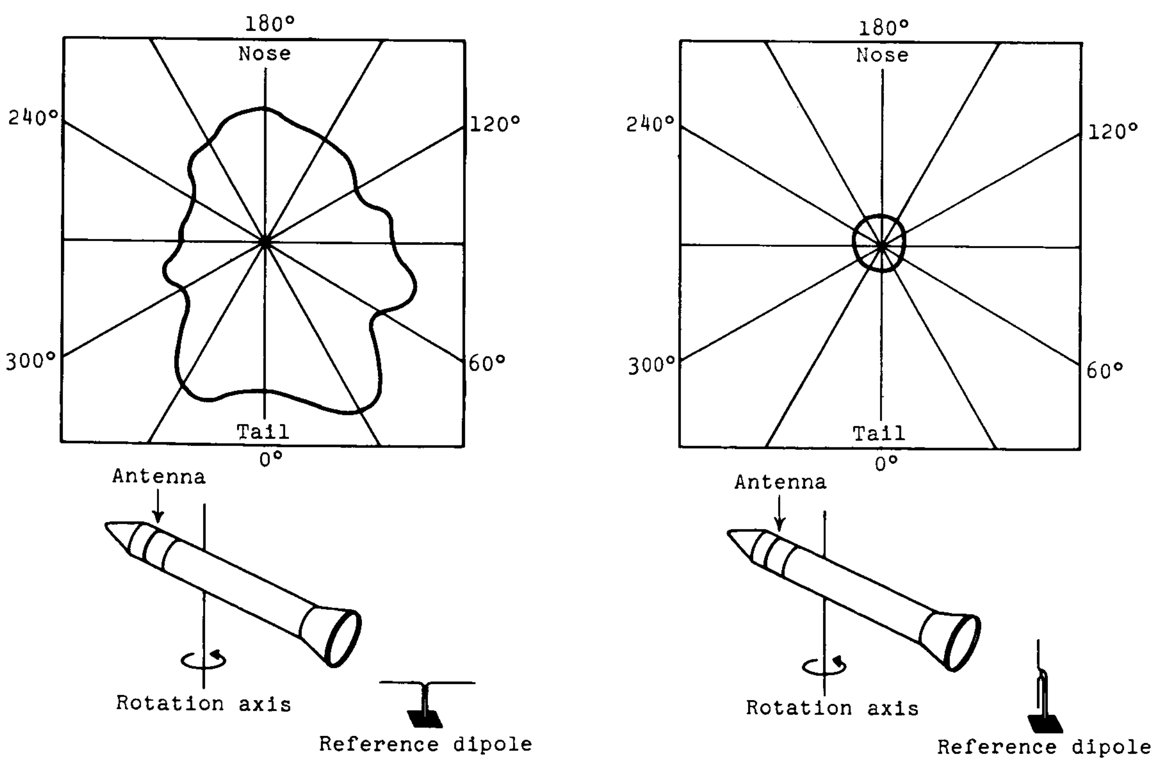

Figure 5.- Aft-ring-antenna pattern.

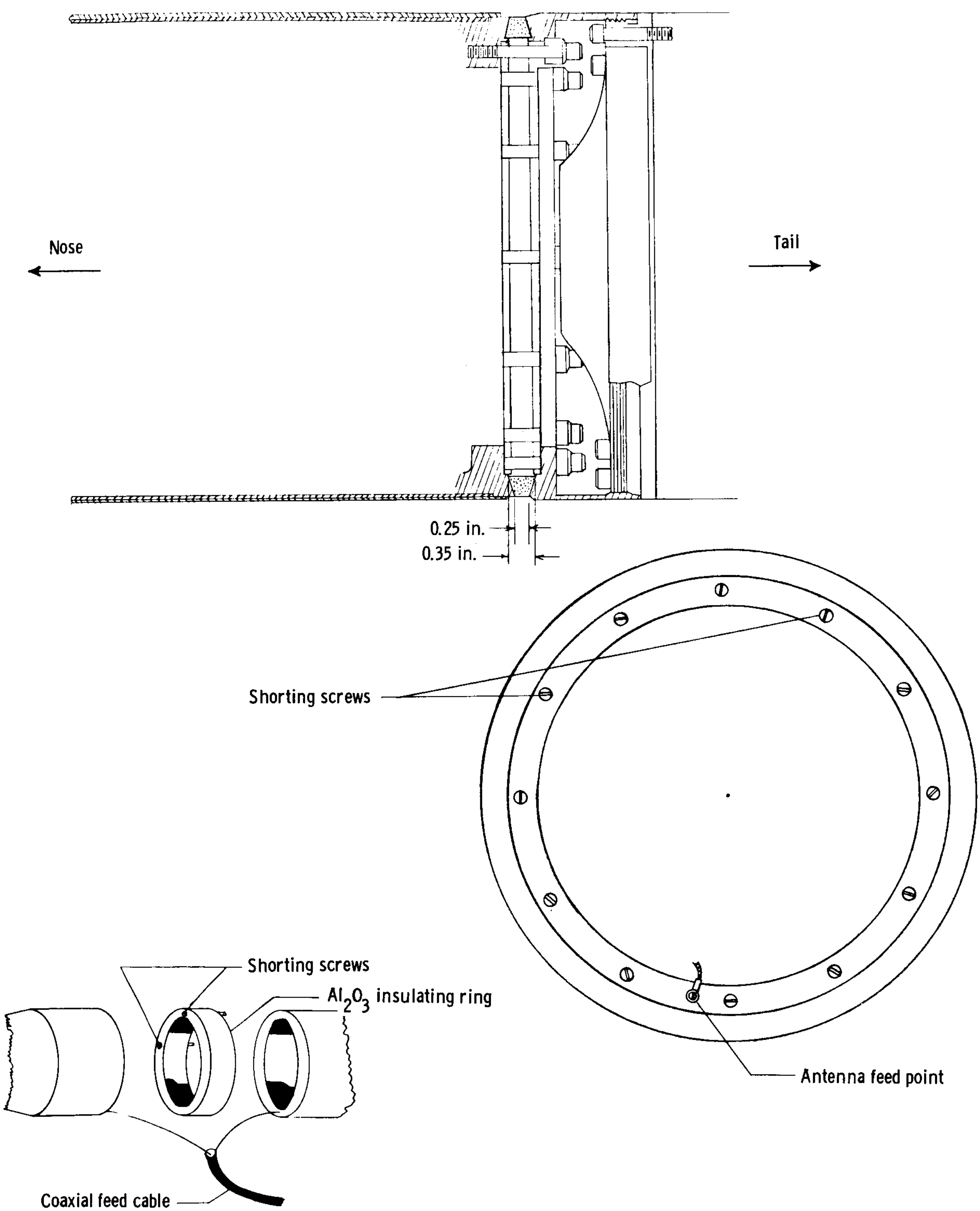

Figure 6.- Detail of aft-ring-antenna construction.

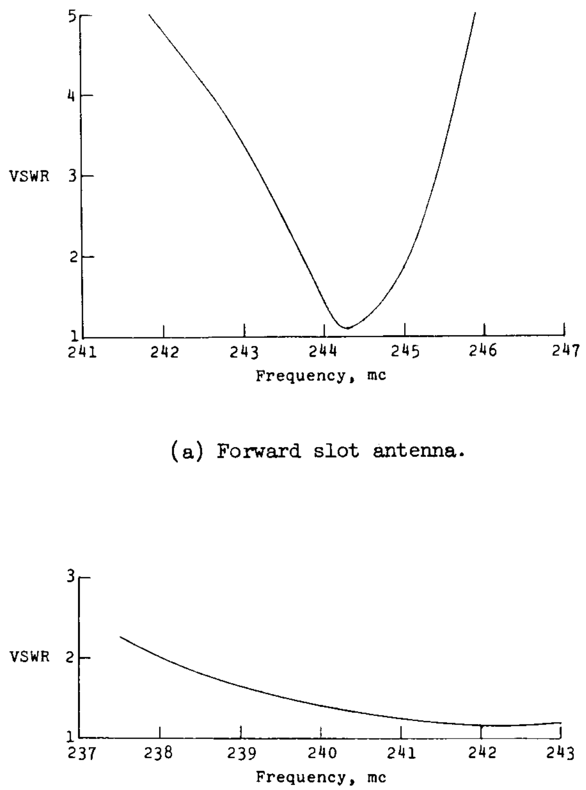

(a) Forward slot antenna.

(b) Aft ring antenna.

Figure 7.- Antenna bandwidth characteristics.

Both crystal-controlled VHF transmitters, the 244.3-mc CW transmitter and the 240.2-mc telemeter transmitter, were of the same design and each had a nominal power output of 2 watts.

The probe was instrumented with an NASA FM/AM telemeter. Measurements obtained from the telemetered data were (1) probe angle of incidence, (2) normal, longitudinal, and transverse accelerations, (3) nose-cone temperatures, (4) CW transmitter forward power, (5) CW transmitter reflected power, and (6) forward-slot-antenna impedance. The first three measurements were made to verify proper vehicle performance and the last three items plus received signal strength were the primary measurements of the experiment.

The forward and reflected powers and the antenna impedance were measured on the transmission line feeding the forward slot antenna as shown in figure 8. The sensor used to measure the forward and reflected powers was a bidirectional coupler with a 40-decibel directivity. The impedance sensor utilized the slotted-line principle and was actually a section of the transmission line. It contained nine detectors spaced equal distances apart and at known distances from the antenna. It was rigidly constructed, was slightly over a half wave length, and was formed into a ring to fit inside the cylindrical body section. The forward and reflected powers and the impedance measurements were made by sampling the detectors and calibration voltages with a commutating switch and telemetering the information to ground receivers on a single telemeter channel. The impedance

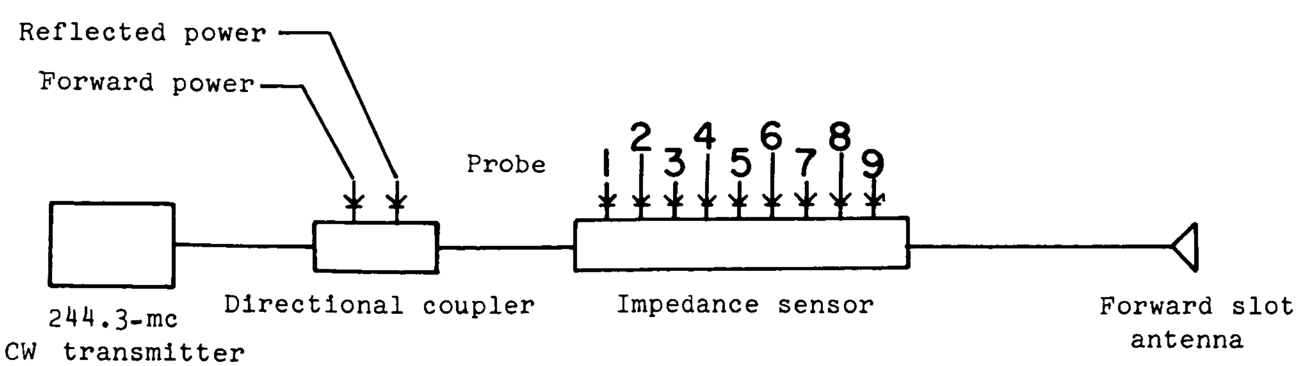

Figure 8.- Transmission line sensors.

detectors were sampled 10 times per second and the bidirectional coupler and calibration voltages were sampled 5 times per second.

Ground Range

The ground range used for the flight is shown in figure 9. The telemeter signal was recorded on magnetic tape at Wallops Station and aboard ship. Signal

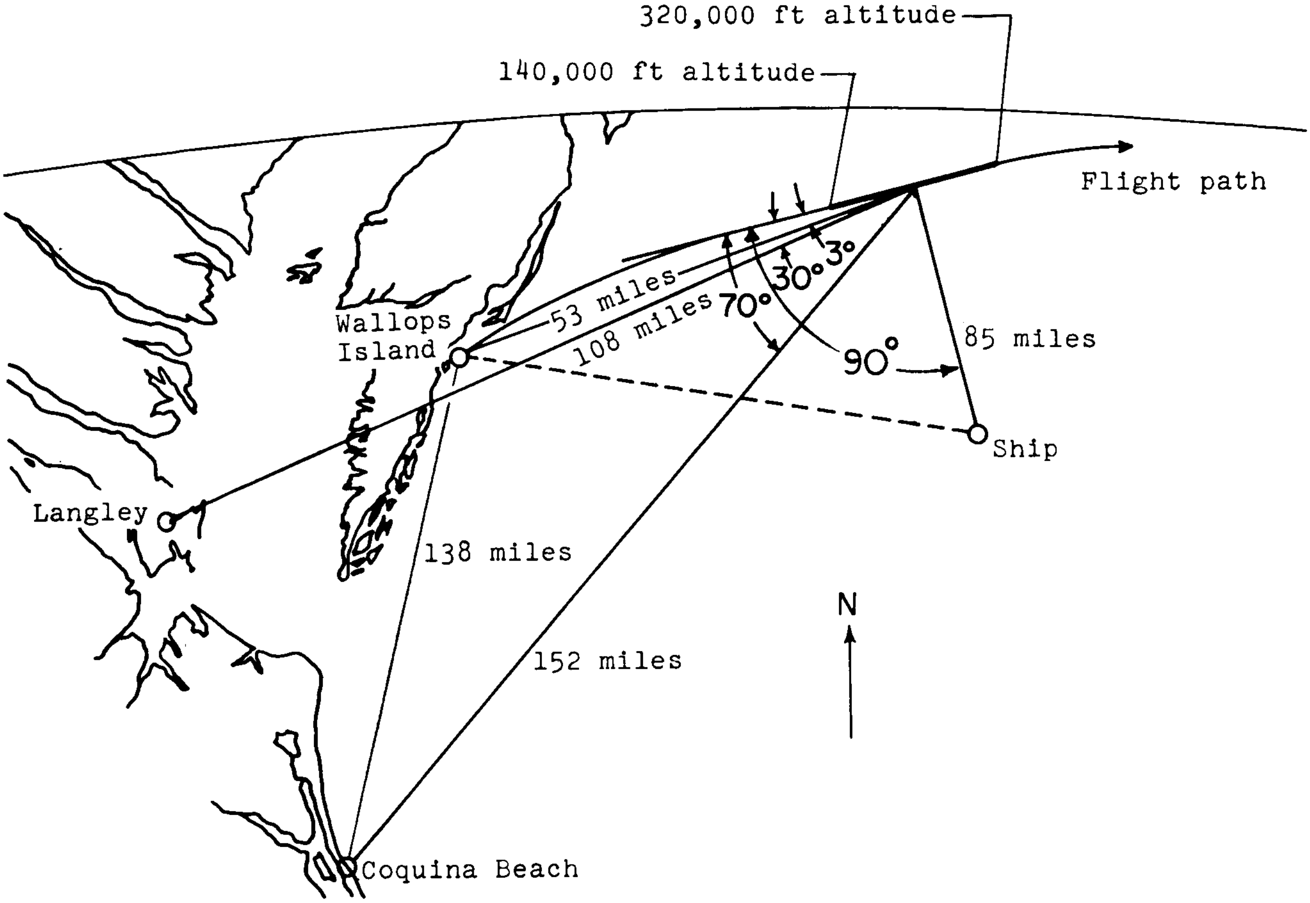

Figure 9.- RAM A1 spatial trajectory during the prime data period as seen from the ground range.

strengths from both VHF antennas were recorded on magnetic tape at Wallops Station, Langley, Coquina Beach on the North Carolina coast, and aboard ship in the Atlantic Ocean. The look angles from the ground receiver sites with respect to the vehicle longitudinal axis were approximately 3° from Wallops, 30° from Langley, 70° from Coquina Beach, and 90° from the ship. These angles remained essentially constant during the prime data period (between 140,000 feet and 320,000 feet). The signal-strength measurements were accomplished by tape recording the automatic gain control voltages from calibrated receivers with voltage-controlled oscillators. Wide-beam helical receiving antennas were used throughout the ground range. Before launch time, antennas were pointed toward the center of the prime data period and receivers were accurately set on frequency. Operators of the ground stations were not permitted to track the antennas nor tune the receivers during the prime data period. This precaution was taken to prevent the presence of artificial variations in the signal-strength records.

TEST RESULTS AND DISCUSSION

Vehicle performance was normal throughout the flight. The planned altitude-velocity profile was flown, nose-cone skin temperatures were less than 750° F, and probe angle of incidence varied from near 0° to 5° during the prime data period. This variation in angle of incidence which was expected had no noticeable effect on the data. Velocity and altitude during the data period are shown in figure 10. See reference 1 for further details on vehicle performance.

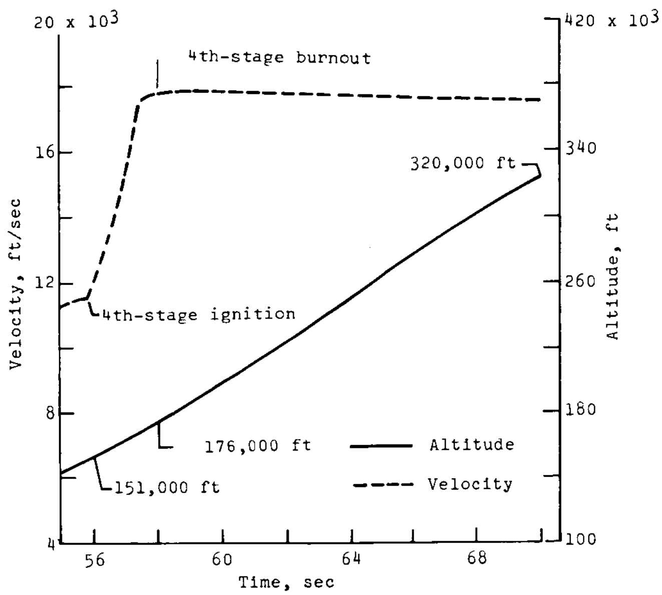

Figure 10.- Time history of velocity and altitude during prime data period.

Signal-strength measurements at Wallops, Langley, Coquina Beach, and the ship for the forward slot antenna are given in figure 11. The signal strengths in decibels are plotted relative to the signal level just prior to fourth-stage ignition. Variances due to spin have been removed by fairing peak values of received signals. The signal started to decrease during fourth-stage burning at an altitude of approximately 156,000 feet and a velocity of 13,000 feet per second and reached a maximum attenuation of 25 decibels at fourth-stage burnout at an altitude of 176,000 feet and a velocity of 17,800 feet per second. All stations indicated approximately the same maximum attenuation. The peak attenuations and curve shapes are very similar at all receiving stations during the period of plasma-sheath interference. This similarity indicates that any antenna-pattern-shape changes were small.

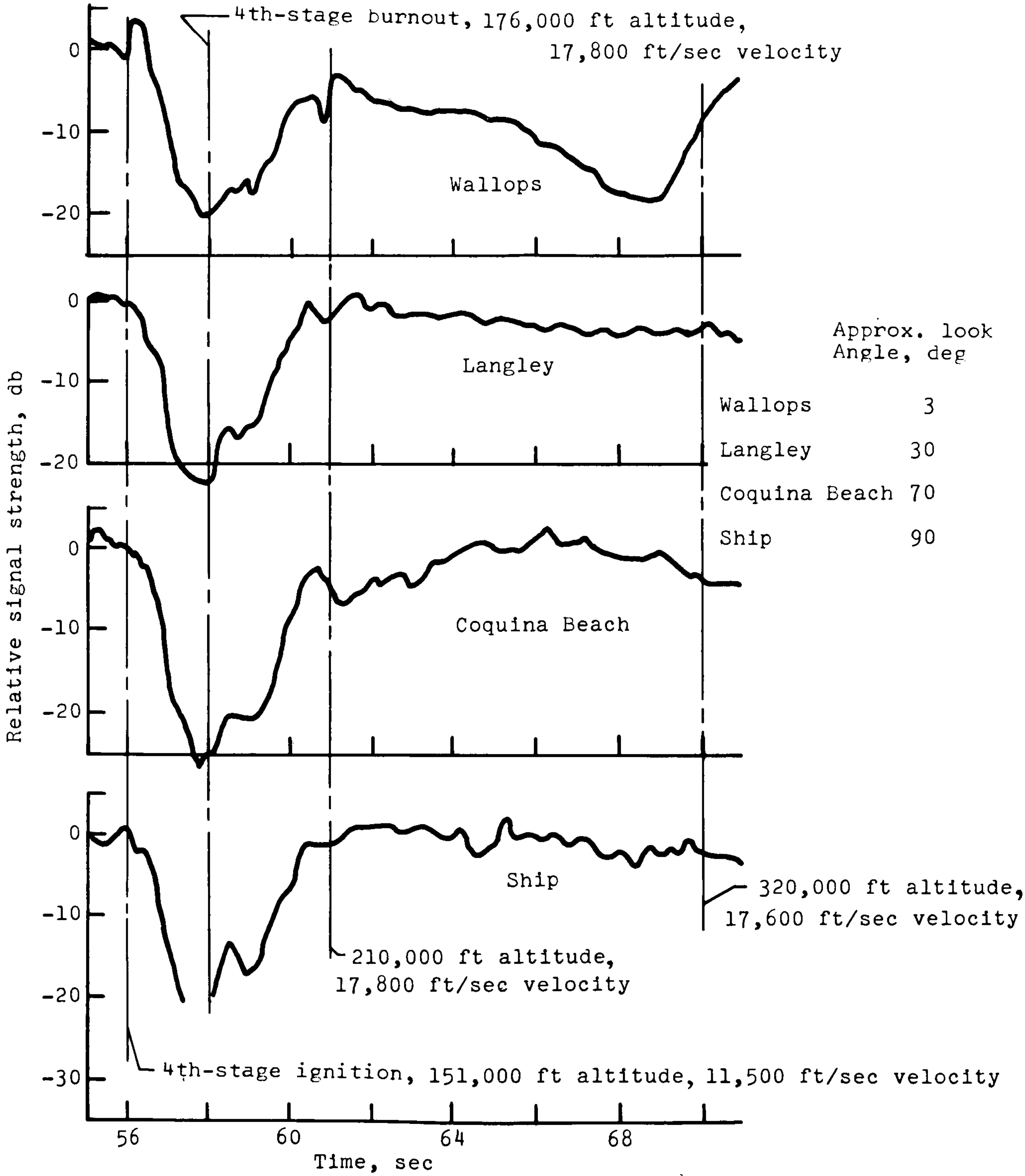

Figure 11.- Received signal strength from forward slot antenna.

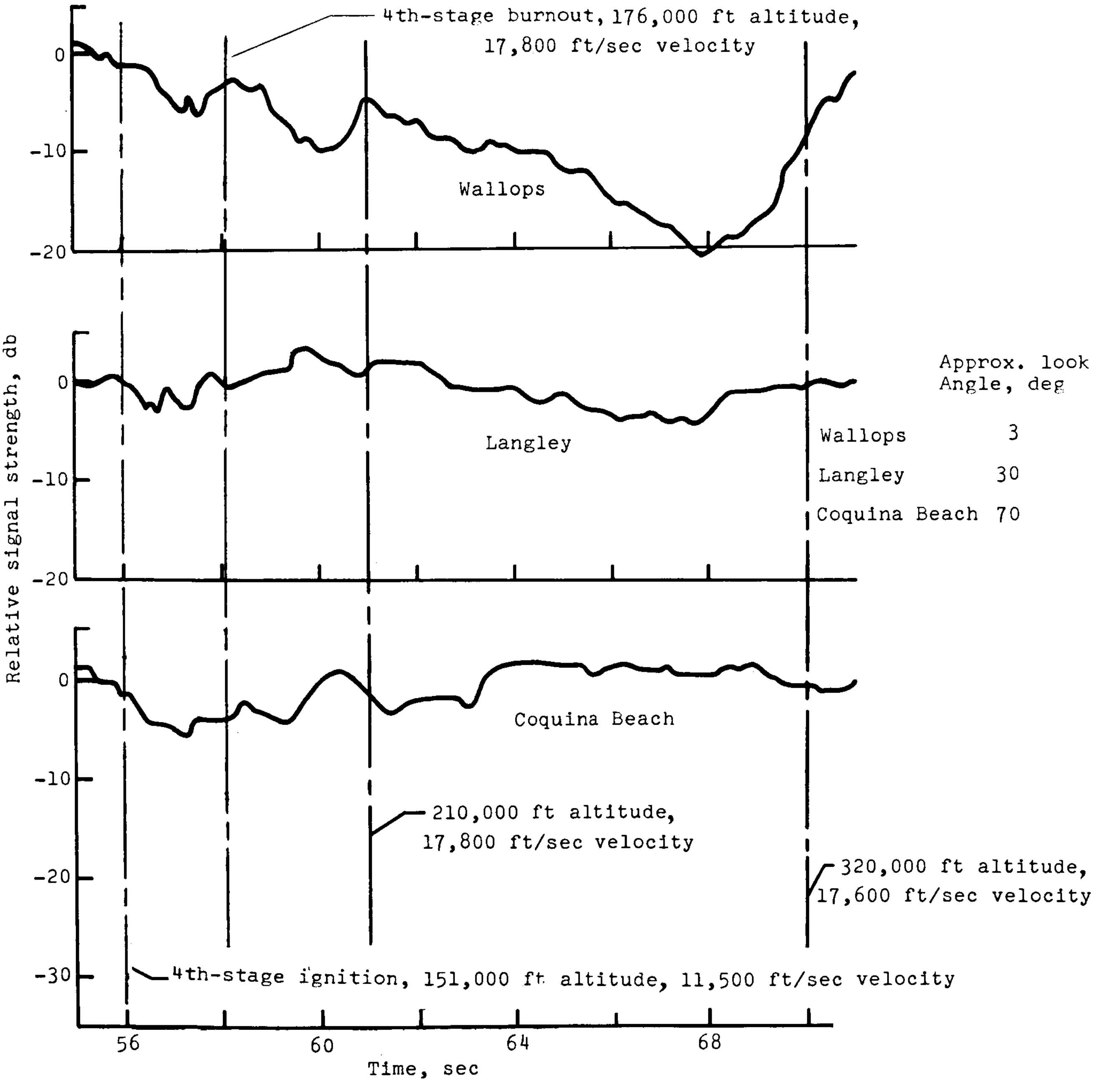

Figure 12.- Received signal strength from aft ring antenna.

Signal-strength measurements at Wallops, Langley, and Coquina Beach for the aft ring antenna are shown in figure 12. Variances in signal strength due to spin have been removed by fairing peak values of received signals. The ship record of this signal was not usable because of inadequate calibrations. Attenuation of this signal during the plasma-sheath-interference period was small for all stations, being no greater than 10 decibels.

It is interesting to note that the exhaust of the burning fourth-stage rocket had no apparent effect on the transmitted signals. There were no sudden changes in signal strength at the various ground stations when the rocket motor ignited nor when it burned out although there might have been some enhancement of attenuation due to flow-field—rocket-exhaust interaction (ref. 3).

During the plasma-sheath-interference period (at altitudes from 156,000 feet to 210,000 feet) the voltage standing-wave ratio (VSWR) on the transmission line feeding the forward slot antenna increased from essentially 1 to a maximum of 8. The VSWR flight measurements are plotted in figure 13. The signal-attenuation

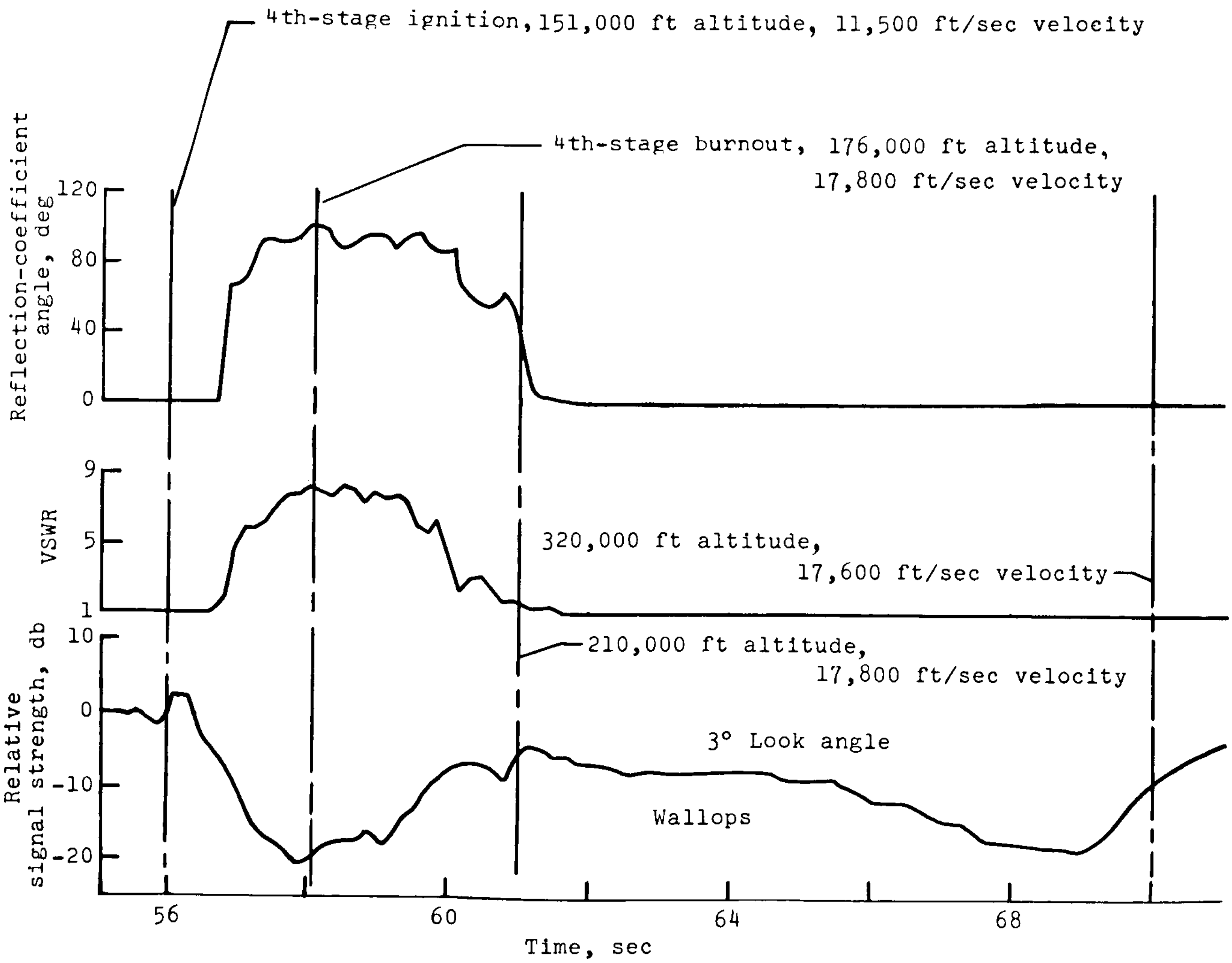

Figure 13.- Reflection-coefficient angle, VSWR, and signal strength for forward slot antenna.

curves plotted in figure 11 are total-signal-loss curves including losses due to antenna mismatch and forward power changes. Forward power fluctuations were negligible and the maximum voltage standing wave ratio of 8 is indicative of a loss of only 4 decibels.

The antenna impedance sensor essentially monitored the voltage standing wave minimum position. The voltage standing wave minimum position is plotted in figure 13 in terms of reflection-coefficient angle. Antenna impedance was calculated for the plasma-sheath-interference period by using the VSWR, the location of the voltage standing wave minimum with respect to the antenna, and a Smith chart. The results, indicating an impedance shift in the inductive direction, are tabulated in table I. Before and after the prime data period the VSWR was near 1 and the impedance was approximately 50 ohms.

TABLE I.- SUMMARY OF FORWARD-ANTENNA-IMPEDANCE MEASUREMENTS

Time, sec	Altitude, ft	Velocity, ft/sec	VSWR	Impedance, ohms
57.0	162,000	15,000	4.5	$62.0\angle 65.0^{\circ}$
57.5	167,000	17,200	6.0	$49.0\angle 71.0^{\circ}$
58.0	173,000	17,750	8.1	$43.0\angle 74.8^{\circ}$
59.0	185,000	17,800	7.8	$47.7\angle 75.4^{\circ}$
59.5	192,000	17,800	5.9	$45.2\angle 70.6^{\circ}$
60.0	198,000	17,800	4.5	$57.0\angle 64.5^{\circ}$
60.5	205,000	17,750	3.1	$52.8\angle 53.4^{\circ}$

Figures 11, 12, and 13 show a rather large drop (a maximum of approximately 20 decibels) in the strength of both VHF signals at Wallops when the probe is in the 300,000-foot-altitude region. No corresponding increase in VSWR and reflection-coefficient angle occurs; this indicates that the antenna was unaffected. It is difficult to visualize antenna pattern changes that would cause the effects noted; therefore, vehicle wake phenomena are suspected. Electron clouds due to hypervelocity vehicles, ionosphere seeding, and flare explosions once formed at high altitudes are known to persist for extended periods because of the slow rate of electron recombination at low pressures (ref. 4).

COMPARISON OF FLIGHT RESULTS WITH THEORETICAL PREDICTIONS

Flight results are compared with theoretical signal-attenuation predictions in figure 14. The figure is prepared for a flight trajectory point near maximum signal loss (altitude of 170,000 feet and a velocity of 17,700 feet per second).

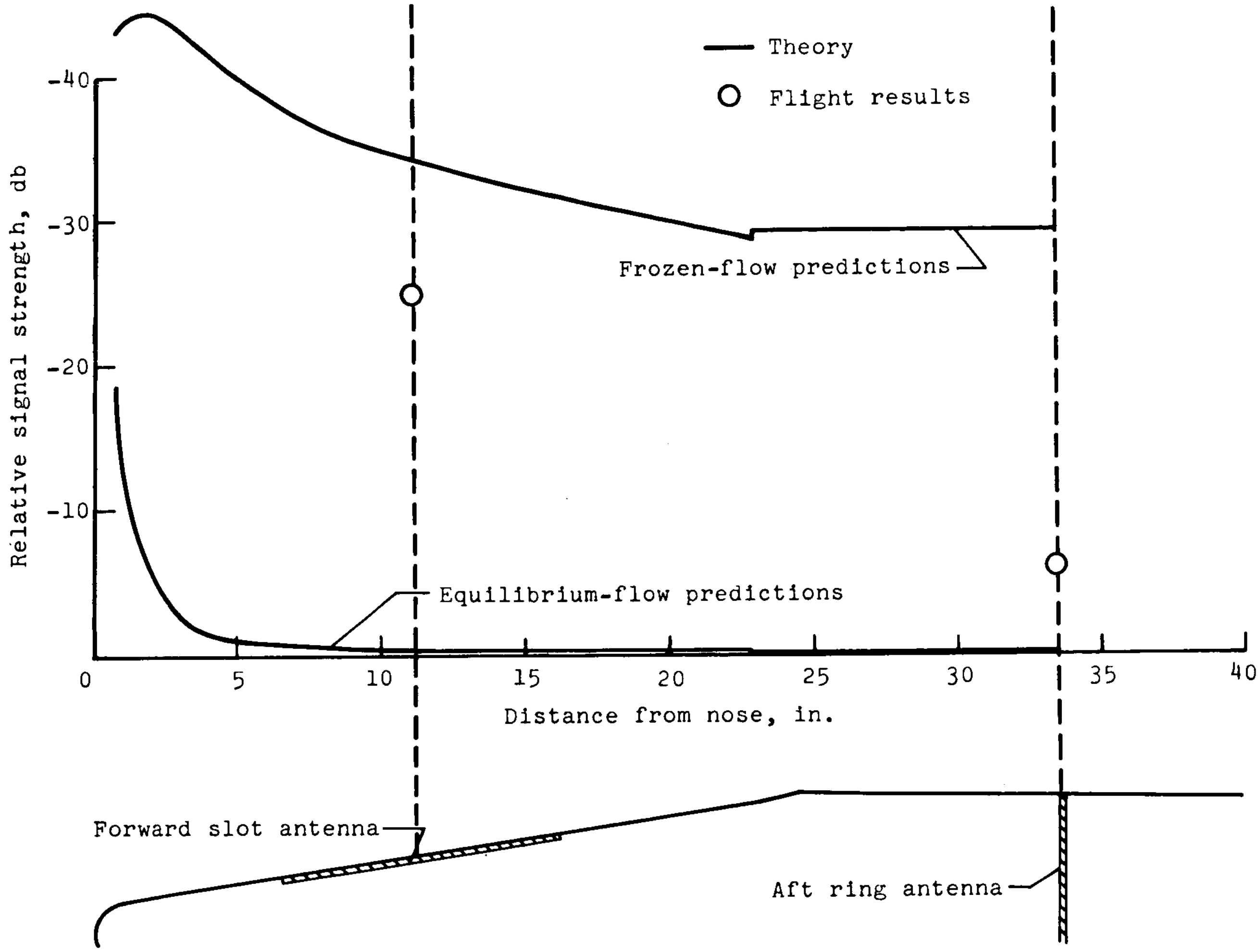

Figure 14.- Comparison of theoretical predictions and flight results at an altitude of 170,000 feet and a velocity of 17,700 feet per second.

Theoretical predictions are given for the two limiting thermochemical-flow models, equilibrium flow and frozen flow (no recombination of atoms or ions) following the shock. The equilibrium predictions were made by using real gas characteristics for a 9° hemisphere-cone body (ref. 5) and the modifications made in reference 6. These modifications were extrapolations to slightly different altitude and Mach number and allowances for the Prandtl-Meyer expansion which occurs at the cone-cylinder juncture of the probe covered by this study. The frozen-flow predictions were made in reference 6 with infinitely slow rates assumed for all chemical reactions after the attainment of complete equilibrium immediately upon crossing the shock front. The signal attenuations for both equilibrium flow and frozen flow were calculated in reference 6 by using available electromagnetic theory with the incident signal assumed to be a plane wave at normal incidence to the plasma sheath.

The results of the comparison made in figure 14 indicate that the flight measurements are in closer agreement with predictions based on the assumption of equilibrium for the aft ring antenna than with those for the forward slot antenna. This comparison points up possible nonequilibrium chemistry in the flow field.

Another explanation is that the large change in decibel loss between the forward and aft antennas could be due to differences in antenna design. Figure 14 shows that for the equilibrium condition predicted losses are essentially the same for both antenna locations. Also, the frozen-flow-field assumption indicates a difference of only a few decibels between the antennas. If identical antennas had been employed, the difference in signal losses should have been quite small in accordance with the approximately equal predicted plasma characteristics at both antennas. As shown in figure 7 the forward antenna is narrow band and the aft antenna is broad band. Therefore, if the plasma environment causes detuning of the antennas, then the aft broad-band antenna would suffer less signal loss.

CONCLUDING REMARKS

A carefully controlled VHF attenuation flight experiment, RAM A1, was conducted in which aerodynamic shaping was utilized to prevent total signal blackout. The measured signal attenuations, a maximum of 25 decibels for the forward slot antenna and of 10 decibels for the aft ring antenna, lie within the predicted bounds according to the two limiting thermochemical-flow models, equilibrium flow and frozen flow. Additional study is indicated to determine the extent of involvement of nonequilibrium chemistry. The voltage standing-wave ratio for the forward slot antenna rose to 8; this indicates a 4-decibel loss due to mismatch. Additional detuning losses related to the antenna bandwidth characteristics are indicated. Differences in signal loss from the forward slot antenna and the aft ring antenna may be due to either nonequilibrium chemistry or antenna bandwidth characteristics. Antenna-pattern-shape changes due to the plasma sheath were small. The forward-slot-antenna impedance shifted in the inductive direction. The exhaust of the burning fourth-stage rocket had no apparent effect on VHF signal levels. Attenuation of the signals received at Wallops Station when the payload stage was in the 300,000-foot-altitude region may be due to wake phenomena.

Langley Research Center,
National Aeronautics and Space Administration,
Langley Station, Hampton, Va., November 20, 1962.

REFERENCES

1. Levine, Jack: Performance and Some Design Aspects of the Four-Stage Solid-Propellant Rocket Vehicle Used in the RAM A1 Flight Test. NASA TN D-1611, 1963.

2. Falanga, Ralph A., Hinson, William F., and Crawford, Davis H.: Exploratory Tests of the Effects of Jet Plumes on the Flow Over Cone-Cylinder-Flare Bodies. NASA TN D-1000, 1962.

3. Sims, Theo E., and Jones, Robert F.: Rocket Exhaust Effects on Radio Frequency Propagation From a Scout Vehicle and Signal Recovery During the Injection of Decomposed Hydrogen Peroxide. NASA TM X-529, 1961.

4. Marmo, F. F., Pressman, J., and Aschenbrand, L. M.: Artificial Electron Clouds - A Systematic Study. Geophys. Corp. of America (Bedford, Mass.), 1960.

5. FitzGibbon, Sheila A.: Real Gas Supersonic Flow Field Solutions in the Shock Layer Around a 9° Sphere-Cone at Mach = 20.4, 21.4 and 21.2. Aerod. Data Memo No. 1:48, Missile and Space Vehicle Dept., Gen. Elec. Co., May 1961.

6. Huber, Paul W., and Evans, John S.: Theoretical Shock-Layer Plasma Flow Properties for the Slender Probe and Comparison With the Flight Results. NASA paper presented at Second Symposium on the Plasma Sheath (Boston, Mass.), Apr. 10-12, 1962.